MODEL–REFERENCE ADAPTIVE CONTROL OF CHAOS IN PERIODICALLY FORCED DYNAMICAL SYSTEMS

Yechiel Crispin and Silvia Ferrari
Department of Aerospace Engineering
Embry–Riddle Aeronautical University
Daytona Beach, FL 32114
e–mail: crispinj@db.erau.edu

Abstract:
A model reference adaptive control method is proposed for controlling chaos in periodically forced dynamical systems. The adaptive control uses proportional, derivative and nonlinear feedback to stabilize a chaotic system about a periodic reference model embedded within the chaotic attractor. As an example, the method is applied to control the chaotic rolling motion of a ship oscillating in regular ocean waves which is modelled by a periodically forced oscillator with a cubic nonlinearity. As the wave amplitude increases, the oscillations of the ship undergo a period doubling bifurcation route to chaos, followed by a crisis (capsizing). It is shown that the control system stabilizes the chaotic motion and prevents capsizing at higher wave amplitudes. The power spectral density of the respective time series and the Poincare map technique are used to study the behavior of the chaotic uncontrolled system and the stabilized periodic controlled system.

I. Introduction:

The suppression of chaos in nonlinear dynamical systems is presently a topic of intense research due to its potential applications in many fields. These include nonlinear aerolasticity problems [Virgin and Dowell, 1992], control of chaos in chemical reactions, such as the Belousov–Zhabotinsky reaction–diffusion system [Schwartz and Triandaf, 1994], control of unstable modes in multimodes lasers [Colet, 1994] and many other applications. Recently the problem of chaos control of a forced nonlinear oscillator, such as the problem of ship capsize has been studied by Ding, Ott and Grebogi [Ding, 1994] using the discrete control method of Ott, Grebogi and Yorke (OGY), see for example [Ott, 1990] and the review of [Ott and Spano, 1995]. The OGY method uses the Poincare map and consists of applying small discrete disturbances to stabilize the chaotic system about an unstable periodic orbit. Ding, Ott and Grebogi [Ding, 1994] achieve the suppression of chaos and prevention of the subsequent crisis by adding a discrete control to the periodic forcing of the waves. The control is a small balancing force, compared to the force produced by the waves, and can be implemented by the use of shifting ballasts installed in the ship.

In this paper, a different method for suppressing chaos is proposed. It is a continuous feedback control method which also helps delay the crisis, thus stabilizing the system about an unstable limit cycle, see also some preliminary work in [Crispin and Ferrari, 1995] and a discrete feedback control method for maps [Crispin and Marduel, 1996]. The method is based on the principle of the model reference adaptive control [Astrom, 1995] in which the required behavior is prescribed by a target dynamical reference model. In order to force the controlled system to behave like the target prescribed model, an error function, the difference between the model reference and the controlled system response, is used in the closed loop. Several tools are used in order to investigate the output of the controlled system and distinguish between chaotic and periodic responses. These include the time series and the phase portrait, the power spectrum [Hilborn, 1994] and the Poincare map [Moon, 1992]. The present method can be applied to higher order systems since the method uses continuous feedback control and is not a discrete method based on the Poincare map.

In order to validate the present approach, the method was applied to the problem of chaotic ship oscillations and capsizing. The background of this important problem will be described first. When a ship is subjected to ocean lateral waves of increasing amplitude, the motion of the ship follows a period–one limit cycle oscillation. When the amplitude of the waves increases, a period doubling bifurcation occurs. A further increase of the forcing amplitude produces a period doubling cascade which leads to chaotic motion. Beyond a critical value of the forcing amplitude, the ship response escapes from the chaotic attractor, its amplitude increases monotonically and the ship capsizes, a phenomenon known as a crisis. Several authors have treated the problem of forced nonlinear oscillations of a ship in lateral ocean waves [Nayfeh, 1990; Ding, 1994; Thompson, 1990, 1993; Virgin, 1987]. For instance, a nonlinear oscillator with a quadratic non–linearity was used by [Thompson, 1990, 1993]

in order to study ship stability criteria. It was found that in ship capsizing, there is a sudden reduction in the area of the safe basin of attraction in the space of the initial conditions. Nayfeh and Sanchez [Nayfeh, 1989] derive a similar equation of motion with both cubic and quintic nonlinearities. They use a perturbation technique to obtain approximate periodic solutions. By perturbing the relative roll angle with an infinitesimal disturbance, the stability of the approximate periodic solutions is studied using Floquet theory. Parameter ranges for which instability and crisis occur are investigated to provide the designer with a set of initial conditions which lead to capsizing. A similar nonlinear model was used by [Virgin, 1987] to study the response and stability of the ship. A numerical scheme was used to obtain chaotic solutions and the possibility of capsize.

The above mentioned works, with the exception of the paper by Ding, Grebogi and Ott [Ding, 1994], concentrated on the analysis of periodic and chaotic responses, but the possibility of actively controlling chaos and preventing ship capsizing was not attempted. It is in this direction that the present investigation is concentrated in this paper. In section II, the periodic reference model embedded within the chaotic response is described. In section III, the model reference feedback adaptive control method for the suppression of chaos and stabilization of ship capsizing is introduced. Results about the successful suppression of chaos and prevention of ship capsizing for a specific set of ship parameter values are then presented in section IV, V and VI, which are then followed by a summary and conclusions.

II. The Reference Model

Following the model introduced by Ding, Grebogi and Ott [Ding, 1994], the uncontrolled nonlinear oscillator used to describe the motion of the ship is given by the following nonlinear second order ordinary differential equation of the Duffing type:

$$(1)\quad x'' + \nu x' + \omega_0^2 x - \alpha\omega_0^2 x^3 = f(t)\, f_0 \sin\Omega t$$

where x is the angle between the ship mast and the vertical direction, ν is the friction damping coefficient, ω_0 is the natural frequency and α is a parameter characterizing the strength of the nonlinearity. The forcing function $f_0\, f(t) \sin\Omega t$, represents the moment exerted by the waves on the ship. We study the case where the waves magnitude increases slowly over a transient period of time, after which it reaches a constant value f_0. f(t) is a linear function of time that increases from 0 to 1 over a specified transient period and remains equal to 1 thereafter. Ω is the angular frequency of the waves and the primes denote time derivatives. In order to control the chaotic behavior of the system described by Eq.(1), a model reference adaptive system (MRAS) is used. This control system is described in Section III. The required ideal performance of the system is prescribed by a reference model, the target model, which has a required regular period–one response denoted by $x_m(t)$. It is obtained from Eq.(1), by seeking an approximate periodic solution using the method of averaging. This method is documented in the nonlinear oscillations literature [Nayfeh and Mook, 1979], [Hagedorn, 1988], and is given here in outline form. The assumption is that the response is basically sinusoidal, but with the amplitude and phase varying slowly as a function of time. To this extent, one can define the following transformation [Hagedorn, 1988]:

$$(2)\quad x = a(t)\, s(t)$$

$$x' = a'(t)\, s(t) + a(t)\, (\Omega + \theta'(t))\, c(t)$$

where a(t) is the amplitude, $\theta(t)$ is the phase, $s(t) = \sin(\Omega t + \theta)$ and $c(t) = \cos(\Omega t + \theta)$.

x' and x" can be approximated by the following equations :

$$(3)\quad x' \simeq a\, \Omega\, c(t)$$

$$x'' \simeq a'\, \Omega\, c(t) - a\, \Omega\, (\Omega + \theta')\, s(t)$$

where

$$(4)\quad a'(t)\, s(t) + a(t)\, \theta'(t)\, c(t) = 0$$

Substituting the values of x, x' and x", given by Eqs. (2) and (3) in Eq. (1) and rearranging, the following system of equations is obtained:

$$(5)\quad a'\, \Omega = (\Omega^2 - \omega_0^2)\, a\, s(t)\, c(t) - \nu\, a\, \Omega\, c^2(t) + \alpha\, \omega_0^2\, a^3\, s^3(t)\, c(t) + c(t)\, f_0 \sin\Omega t$$

$$a\, \Omega\, \theta' = -(\Omega^2 - \omega_0^2)\, a\, s^2(t) + \nu\, a\, \Omega\, c(t)\, s(t) - \alpha\, \omega_0^2\, a^3\, s^4(t) - s(t)\, f_0 \sin\Omega t$$

Eq. (5) is equivalent to Eq. (1), both systems are second order ordinary differential equations with a time–dependent forcing function. Therefore, both systems are equivalent to a third order autonomous system of ODEs, and therefore they are both able to display chaotic behavior. The model reference system is defined by taking the mean values of the right hand sides of the system of Eqs.(5), over one period:

(6) $\Omega\, a_m' = -\nu\Omega\, a_m - 1/2\, f_0 \sin\theta_m$
$\Omega\, a_m\, \theta_m' = -1/2\,(\Omega^2 - \omega_0^2)\, a_m - 3/8\,\alpha\,\omega_0^2\, a_m^3 - 1/2\, f_0 \cos\theta_m$

where the subscript m indicates the variables of the reference model. Eq. (6) is an autonomous second order system which cannot display chaos. The state variables of the reference model are then given by:

(7) $x_m = a_m(t) \sin(\Omega t + \theta_m)$

$x_m' = a_m\, \Omega \cos(\Omega t + \theta_m)$

The solution of Eqs.(6,7), the model reference system, with initial conditions $a_m(0) = 0$, $\theta_m(0) = 0$ and parameter values $\nu = 0.5$, $\omega_0 = 1$, $\alpha = 1$ and $f_0 = 0.72$, is shown in Fig.1. Fig.1(a) shows the time series and Fig.1(b) shows a limit cycle in the phase plane. The parameters of the model were chosen to be equal to the uncontrolled system parameters. The amplitude of the waves is growing from zero at t = 0 to one at t = 50 and remains constant thereafter. The oscillations of the reference model are following the behavior of the forcing waves. For $t > 50$, the oscillations approach the ideal stable period–one limit cycle shown in the figure.

III. Model–Reference Adaptive Control of Chaos and Crisis:

The model reference adaptive control system is characterized by two loops: a feedback inner loop, which includes the system (process) and the regulator, and an outer loop, which serves to adjust the inner loop control parameters. An adjustment mechanism in the inner loop follows the error $e = x_m - x$ and modifies the regulator parameters accordingly. Define an error e(t), the deviation of the controlled system response from the reference model :

(8) $e = x_m - x;\quad e' = x_m' - x';\quad e'' = x_m'' - x''$

Using the error e, the following closed loop controlled system is proposed:

(9) $x'' + \nu x' + \omega_0^2 x - \alpha\omega_0^2 x^3 = K_p\, e + K_d\, e' + K_n\, e^3 + f(t)\, f_0 \sin\Omega t$

where K_p, K_d and K_n are control gains to be adjusted such as to decrease the error e. As the dynamics of the controlled system start locking on the dynamics of the reference model, the proportional, derivative and nonlinear controls $K_p\, e$, $K_d\, e'$ and $K_n\, e^3$, respectively, become small, thus reducing the control effort. We study the set of parameters given by [Ding, 1994], namely, $\nu = 0.5$, $\omega_0 = 1$, $\alpha = 1$ and $f_0 > 0.7$. Using Eq. (8), Eq. (9) can be written as:

(10)
$x'' + (\nu + K_d)x' + (\omega_0^2 + K_p + 3\, K_n\, x_m^2)x - 3\, K_n\, x_m\, x^2 - (K_n + \alpha\omega_0^2)x^3 = K_p\, x_m + K_d\, x_m' + K_n\, x_m^3 + f(t)\, f_0 \sin\Omega t$

From the new coefficients appearing in Eq.(10), it can be seen that the effective physical parameters of the controlled system can be varied by applying the control gains K_p, K_d and K_n. The control problem now is to vary the gains such as to minimize the error e(t). For this purpose, an objective function J is defined as:

(11) $J(K_p, K_d, K_n) = e^2 / 2$

In order to minimize e, the control gains are adjusted so that their magnitude is proportional to the negative direction of the gradient of J as will be shown below. The derivatives of J with respect to the controls K_p, K_d and K_n are evaluated as follows:

(12)
$dJ/dK_p = e\, de/dK_p = e\,(dx_m/dK_p - dx/dK_p)$
$dJ/dK_d = e\, de/dK_d = e\,(dx_m/dK_d - dx/dK_d)$
$dJ/dK_n = e\, de/dK_n = e\,(dx_m/dK_n - dx/dK_n)$

The sensitivity functions S_p, S_d and S_n are defined by the following equations:

(13)
$S_p = de/dK_p = dx_m/dK_p - dx/dK_p$
$S_d = de/dK_d = dx_m/dK_d - dx/dK_d$
$S_n = de/dK_n = dx_m/dK_n - dx/dK_n$

Since the reference model x_m is independent of the gains K_p, K_d and K_n, Equations (12,13) reduce to:

(14)
$dJ/dK_p = e\, S_p = e\,(-dx/dK_p)$
$dJ/dK_d = e\, S_d = e\,(-dx/dK_d)$
$dJ/dK_n = e\, S_n = e\,(-dx/dK_n)$

From Eq.(13), it follows that:

(15)
$de'/dK_p = dS_p/dt = S_p'$
$de''/dK_p = d^2S_p/dt^2 = S_p''$

Similar equations are obtained for S_d and S_n. The periodic model reference satisfies Eq.(1), i.e.:

(16) $x_m'' + \nu x_m' + \omega_0^2 x_m - \alpha\omega_0^2 x_m^3 = f(t)\, f_0 \sin\Omega t$

Subtracting Eq.(9) from the model reference Eq.(16), the following equation for the evolution of the error e(t) is obtained:

(17) $e'' + (\nu + K_d)\, e' + (\omega_0^2 + K_p)\, e + K_n\, e^3 - \alpha\omega_0^2\,(x_m^3 - x^3) = 0$

The governing equations for the sensitivity functions are found from equations (13), (15) and (17):

(18)
$$S_p'' + AS_p' + BS_p = -e$$
$$S_d'' + AS_d' + BS_d = -e'$$
$$S_n'' + AS_n' + BS_n = -e^3$$

where

$$A = \nu + K_d$$
$$B = \omega_0^2 - 3\,\alpha\,\omega_0^2\,x^2 + K_p + 3\,K_n\,e^2.$$

In order to minimize the objective function J, the control gains K_p, K_d, and K_n are varied in the direction of the negative gradient of J [Astrom, 1995]:

(19)
$$dK_p/dt = -\gamma_p\, dJ/dK_p = -\gamma_p\, e\, de/dK_p$$
$$dK_d/dt = -\gamma_d\, dJ/dK_d = -\gamma_d\, e\, de/dK_d$$
$$dK_n/dt = -\gamma_n\, dJ/dK_n = -\gamma_n\, e\, de/dK_n$$

From Eqs. (13) and (19), the governing equations for the evolution of the control gains are obtained:

(20)
$$K_p' = -\gamma_p\, S_p\, e$$
$$K_d' = -\gamma_d\, S_d\, e$$
$$K_n' = -\gamma_n\, S_n\, e$$

where γ_p, γ_d and γ_n are constants to be adjusted. If the values of γ's are too low, the chaotic behavior cannot be controlled and the closed loop system might become unstable. If the chosen values of the γ's are too high, the control gains K_p, K_d and K_n could become too high, which is also undesirable, since the invested control effort should be kept low. It was found that a value of $\gamma_p = \gamma_d = \gamma_n = 0.02$ is a good compromise between the two requirements. In the simulations, Eqs.(6,7) for the reference model, Eq.(10) for the closed loop adaptive controlled system, Eqs.(18) for the sensitivity functions and Eqs.(20) for the control gains are solved simultaneously using a fourth order Runge–Kutta method with variable step size. The initial conditions used in the simulations are discussed in the next section.

IV. Time Series and Phase Portraits of the Controlled and Uncontrolled Systems:

In order to study the uncontrolled nonlinear system, Eq.(10) was solved with no controls applied, i.e. with $K_p = 0$, $K_d = 0$ and $K_n = 0$. The time series for this system is shown in Fig.2(a) for an amplitude $f_0 = 0.72$. It can be seen that the time series is chaotic. Next the adaptive feedback control was applied to the same system with the same amplitude of the forcing waves $f_0 = 0.72$. The controlled system is simulated by solving the system of equations (6), (7), (10), (18) and (20) with the initial conditions $a_m(0) = 0$, $\theta_m(0) = 0$, $x(0) = 0$, $x'(0) = 0$, $S_p(0) = 0$, $S_p'(0) = 0$, $S_d(0) = 0$, $S_d'(0) = 0$, $S_n(0) = 0$ and $S_n'(0) = 0$. The initial conditions for the adaptive gains were taken as $K_p(0) = K_d(0) = K_n(0) = 0$. The time series of the controlled system is given in Fig.2(b). It can be seen that the response converges to a period–one limit cycle as compared to the uncontrolled chaotic signal. Fig.3 shows the behavior of the uncontrolled and the controlled systems in the phase plane. For the uncontrolled system, the phase portrait is a chaotic attractor (the oscillator cycle does not repeat itself). On the other hand, when the adaptive feedback control is applied, the chaotic oscillations are suppressed and the trajectory approaches a limit cycle. A similar result can be seen in Fig.4 where the error e, i.e. the difference between the model reference response x_m and the system response x, is displayed for the uncontrolled and the controlled systems. The chaotic error of the uncontrolled system is reduced to a periodic error of much smaller amplitude.

The proportional sensitivity and control functions are shown in Fig.5. It can be seen that both signals are periodic and have a small amplitude. In particular the control is three orders of magnitude smaller than the controlled signal, which means a relatively small effort is needed in order to stabilize the system. The periodicity of the proportional control indicates that the error function is also periodic and, thus, that the system has been stabilized. From Fig.6 it can be seen that the derivative sensitivity and the derivative control also approach periodic behavior and their magnitude is small compared to the controlled system response. The nonlinear sensitivity and control were found to be very small and displayed a similar behavior as in Figs. 5 and 6.

V. Poincare Maps and Power Spectrum of the Controlled and Uncontrolled Systems

Poincare maps were obtained for both the controlled and the uncontrolled systems in order to distinguish between the periodic behavior of the controlled system and the chaotic behavior of the uncontrolled system. The equations of motion are solved using a variable step Runge–Kutta fourth order integration scheme. The time series obtained are sampled at discrete time intervals $t_n = n(T/10)$, where $n = 0, 1, 2, \ldots$ and $T = 2\pi$ is the nondimensional period of the waves. The sampled data points are subsequently used in order to obtain the power spectrum density. If the system were perfectly periodic and sampled every full period T, the Poincare map would appear as a single point. The motion may be considered to be chaotic if the map consists of a large set of points which do not repeat or do not

form a closed orbit (as in quasi–periodic motion). In that case, the points define a chaotic attractor.

When the Poincare map displays data that are sampled every T/10 time steps, ten branches appear in the chaotic attractor, each corresponding to a different starting point T/10, 2T/10, 3T/10 etc., as can be seen in Fig.7(a) for the uncontrolled chaotic system. Comparing this result to the Poincare map of the controlled system shown in Fig.7(b), a dramatic difference is observed, showing that the controlled system is clearly periodic, since exactly 10 points are obtained, each corresponding to a different starting point of time T/10, 2T/10 etc., the motion repeating itself every full period T.

An additional tool was used to diagnose the periodic behavior of the controlled system versus the chaotic behavior of the uncontrolled system: the power spectral density. For a description of this technique, see e.g. [Hilborn, 1994]. The basis of the method is an analysis of the frequency content of the sampled signal using the fast Fourier transform (FFT) for which very efficient numerical methods have been developed. The absolute value squared of the fast Fourier transform is considered to be the amount of power contained in the frequency range considered. The spectrum of a chaotic signal is characterized by many irregular peaks of different amplitudes over a wide bandwidth, while the spectrum of a periodic signal would display one main peak and a smooth spectral curve. A comparison of the power spectral densities is shown in Figs.8(a) and 8(b).

The power spectrum of the controlled system is shown in Fig.8(b). It can be seen that the power spectrum has a main peak, which corresponds to the natural frequency of the system, and by a second peak, having an amplitude about four orders of magnitude smaller than the main peak, which corresponds to an additional frequency superimposed on the main frequency. The power spectrum of the reference model is similar to that of the controlled system, except that it does not display a second peak. from Fig.8(a), it is apparent that the uncontrolled system is clearly chaotic as indicated by the numerous irregular peaks.

VI. Controlling the Crisis (Capsizing)

Previous work [Ding et al, 1994] as well as our simulations have shown that as the amplitude of the waves f_0 increases from zero to 0.7, the motion of the ship follows a period–one limit cycle. When the amplitude is increased further, the motion undergoes a period doubling bifurcation route to chaos which persists up to an amplitude value around 0.726. When the amplitude is increased beyond this critical value, the chaotic oscillations lead to a crisis, the amplitude of the motion increases indefinitely, which signals the capsizing of the ship. This crisis phenomenon is shown in Fig.9(a) for the uncontrolled system for an amplitude of 0.78 which is beyond the critical value. Applying the feedback adaptive control stabilizes the ship motion and suppresses chaotic oscillations as shown in Fig.9(b). The controlled periodic motion is maintained well beyond the time for the onset of the crisis. This can also be seen from the phase portrait of the two systems as shown in Fig.10. The motion of the uncontrolled system escapes the attractor, following an oscillatory transient period. Fig.10 also shows that by using the present adaptive control scheme, the crisis can be stabilized around the reference model limit cycle.

Conclusions:

A continuous model reference adaptive feedback control method is proposed for the suppression of chaos in periodically forced dynamical systems. As an example, an application of the control system to the response of a ship oscillating in lateral ocean waves is studied. The control law consists of proportional, derivative and nonlinear feedback. A periodic reference model obtained from the ship equation of motion by the method of averaging is presented. It was found that for forcing amplitudes below the capsize critical value, suppression of chaos is achieved, and the response follows the ideal model reference period–one limit cycle. For forcing amplitudes above the capsize critical value, ship capsizing is avoided and the crisis is stabilized. This control method is also capable of stabilizing the system at higher forcing amplitudes. Several tools are used to diagnose the controlled system periodic behavior and the uncontrolled chaotic response. These include time series, phase portraits, power spectrum densities and Poincare maps. One advantage of the present method is that it is applicable to the control of chaos in higher order systems. Another advantage is that it does not require a permanent digital computer in the control loop, since the continuous control system can be implemented using analog circuits.

Acknowledgement

This work was funded in part by the Vice President of Academics Fund, Embry–Riddle University. The support of the Fund is gratefully acknowledged.

References:

Astrom K.J. and Wittenmark B., Adaptive Control, Addison–Wesley, 1995.

Chacon R., "Inhibition of Chaos in Hamiltonian Systems by Periodic Pulses", Physical Review E, **50**, 750, 1994.

Chacon R., "Suppression of Chaos by Selective Resonant Parametric Perturbations", Physical Review E, **51**, 761, 1994.

Colet P., Roy R. and Wiesenfeld K., "Controlling Hyperchaos in a Multimode Laser Model", Physical Review E, **50**, 5, 3453–3457, 1994.

Crispin Y. and Ferrari S., "Adaptive Control of Chaos Induced Capsizing of a Ship", in Intelligent Engineering Systems Through Artificial Neural Networks, **5**, Fuzzy Logic and Evolutionary Programming, C.H. Dagli et. al, Eds., ASME Press, NY, 1995.

Crispin Y. and Marduel C., "Controlling Chaos in Dynamical Systems Described by Maps", in Proceedings of the First International Conference on Nonlinear Problems in Aviation and Aerospace, International Federation of Nonlinear Analysts, Daytona Beach, FL, 1996.

Ding M., Grebogi C. and Ott E., "Crisis Control: Preventing Chaos–Induced Capsizing of a Ship", Physical Review E, **50**, 4228, 1994.

Hagedorn P., Nonlinear Oscillations, Oxford University Press, Second Edition, Oxford, 1988.

Hilborn R. C., Chaos and Nonlinear Dynamics, Oxford University Press, 1994.

Moon F. C., Chaotic and Fractal Dynamics, an Introduction for Applied Scientists and Engineers, J. Wiley & Sons, 1992.

Nayfeh A.H. and Sanchez N.E., "Stability and Complicated Rolling Responses of Ships in Regular Beam Seas", Int. Shipbuild. Prog. **37**, 331, 1990.

Nayfeh A.H. and Mook D.T., Nonlinear Oscillations, John Wiley and Sons, N.Y., 1979.

Ott E., Grebogi C. and Yorke Y.A., Phys. Rev. Lett., **64**, 1196, 1990.

Ott E. and Spano M., "Controlling Chaos", Physics Today, **48**, 34, 1995.

Schwartz I.B. and Triandaf I., "Controlling Unstable Statesin Reaction–Diffusion Systems Modeled by Time Series", Physical Review E, **50**, 4, 2548–2552, 1994.

Thomas W. C. and Schwartz I. B., "Controlling Unstable Steady States Using System Parameter Variation and Control Duration", Physical Review E, **50**, 3410, 1994.

Thompson J.M.T., Rainey R.C., and Soliman M.S., "Ship Stability Criteria Based on Chaotic Transients from Incursive Fractals", Phil. Trans. R. Soc. Lond. A, **332**, 149, 1990.

Thompson J.M.T., "Chaos and Fractal Basin Boundaries in Engineering", in The Nature of Chaos, Tom Mullin, Ed., Oxford University Press, Oxford, 1993.

Virgin L.N., "The Nonlinear Rolling Response of a Vessel Including Chaotic Motions Leading to Capsize in Regular Seas", Applied Ocean Research, **9**, 89, 1987.

Virgin L.N. and Dowell E.H., "Nonlinear Aeroelasticity and Chaos", in Computational Nonlinear Mechanics in Aerospace Engineering, Progress in Astronautics and Aeronautics, S.N. Atluri, Ed., 146, 531–546, AIAA, Washington, DC, 1992.

Wright J. H. G. and Marshfield W. B., "Ship Roll Response and Capsize Behavior in Beam Seas", Trans. of the Royal Institution of Naval Architects, **122**, 129, 1980.

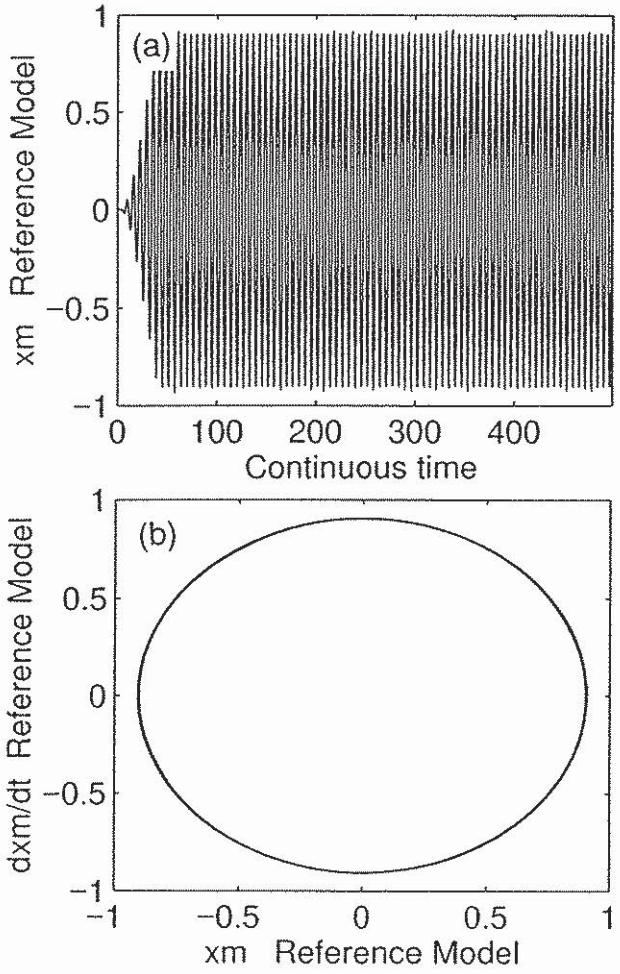

Fig.1: The ideal model reference, (a) its time series and (b) limit cycle.

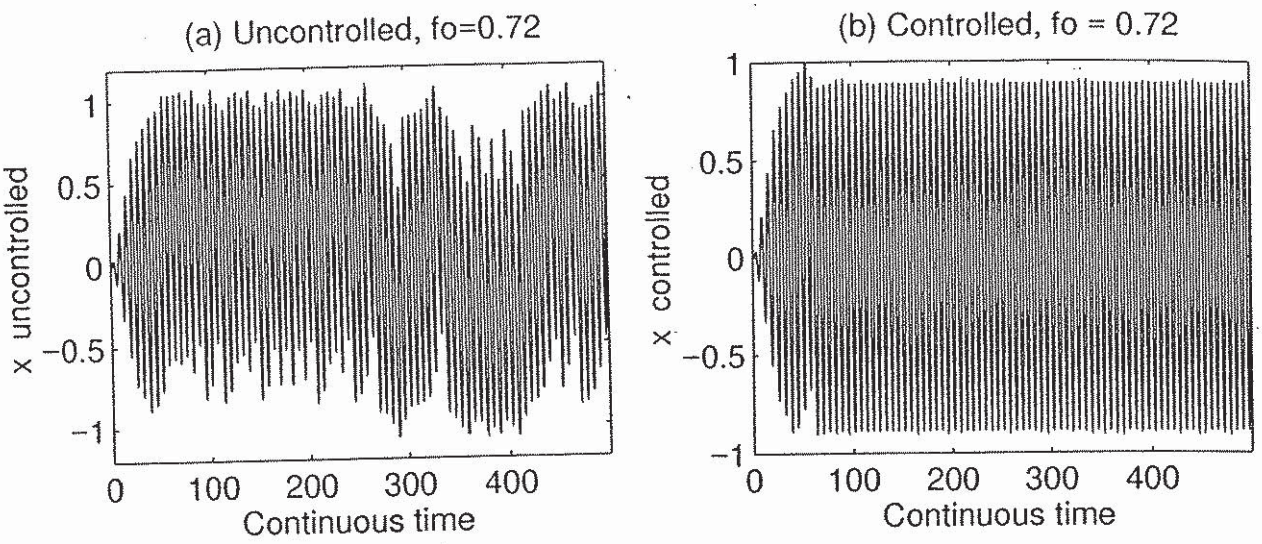

Fig.2: Comparison between (a) the uncontrolled chaotic system and (b) the controlled periodic system.

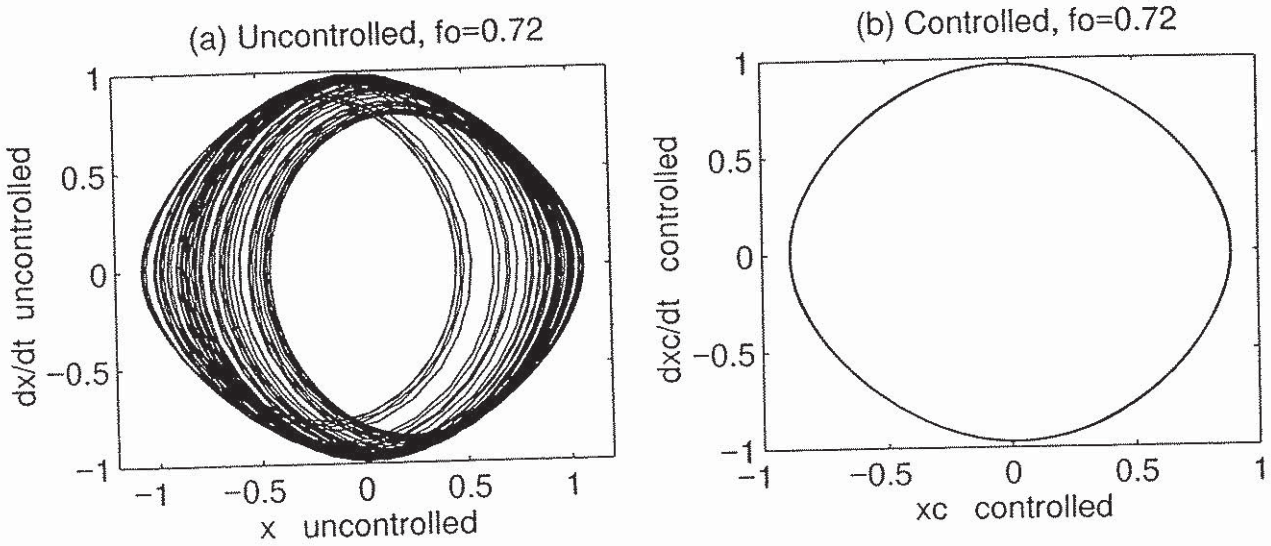

Fig.3: Phase portraits of (a) the chaotic uncontrolled system and (b) the controlled system (limit cycle).

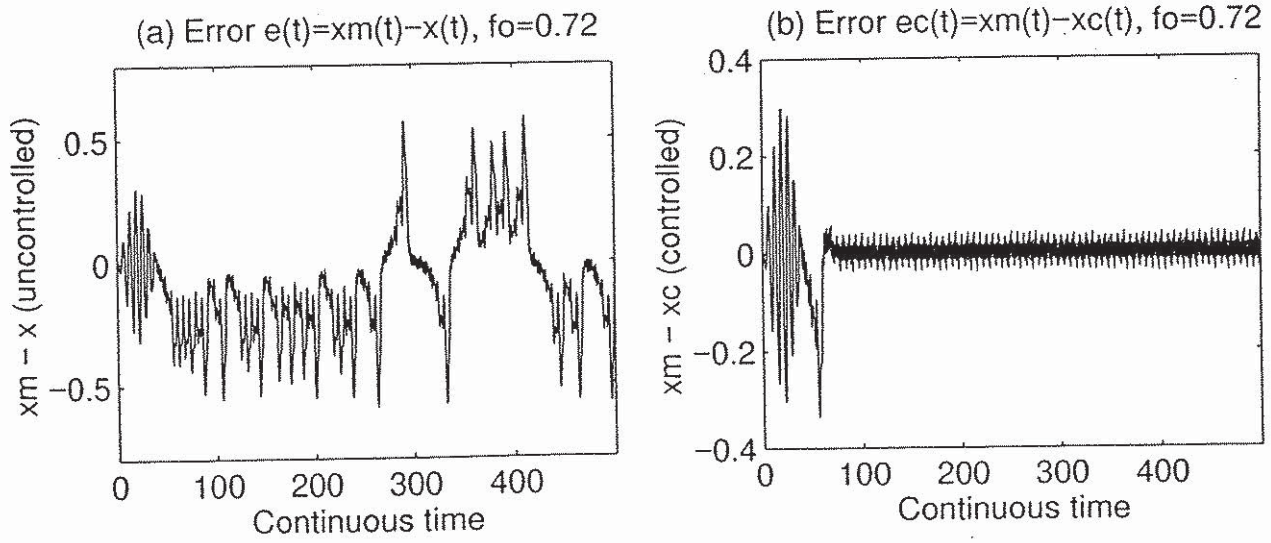

Fig.4: Error function $e(t) = x_m(t) - x(t)$ for (a) the chaotic uncontrolled and (b) the controlled system.

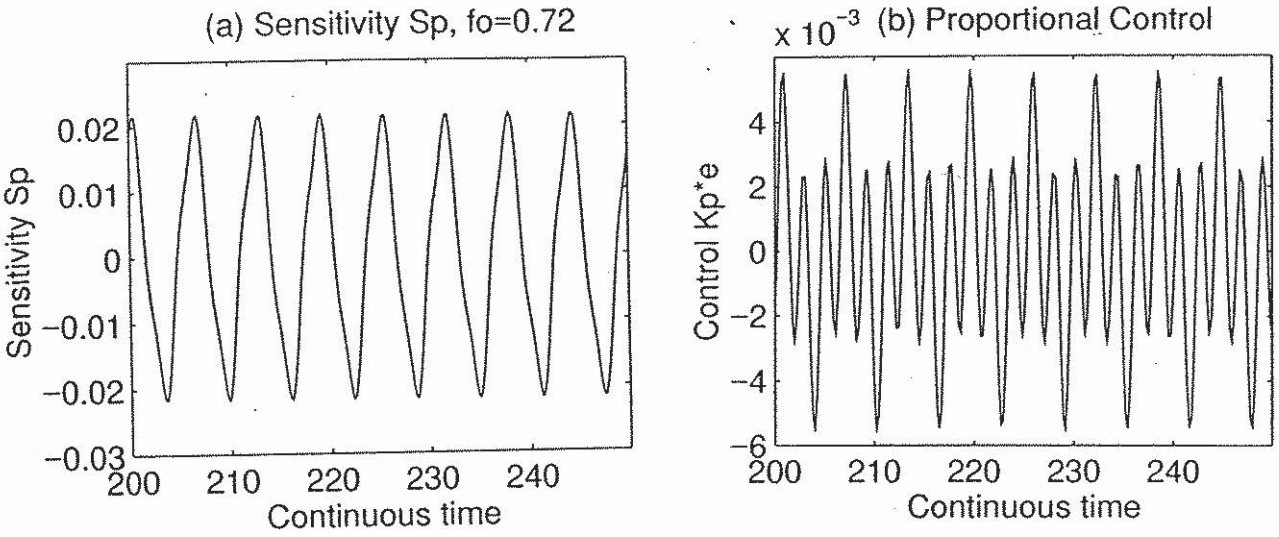

Fig.5: (a) Proportional sensitivity function $S_p(t)$ and (b) the proportional control K_p e.

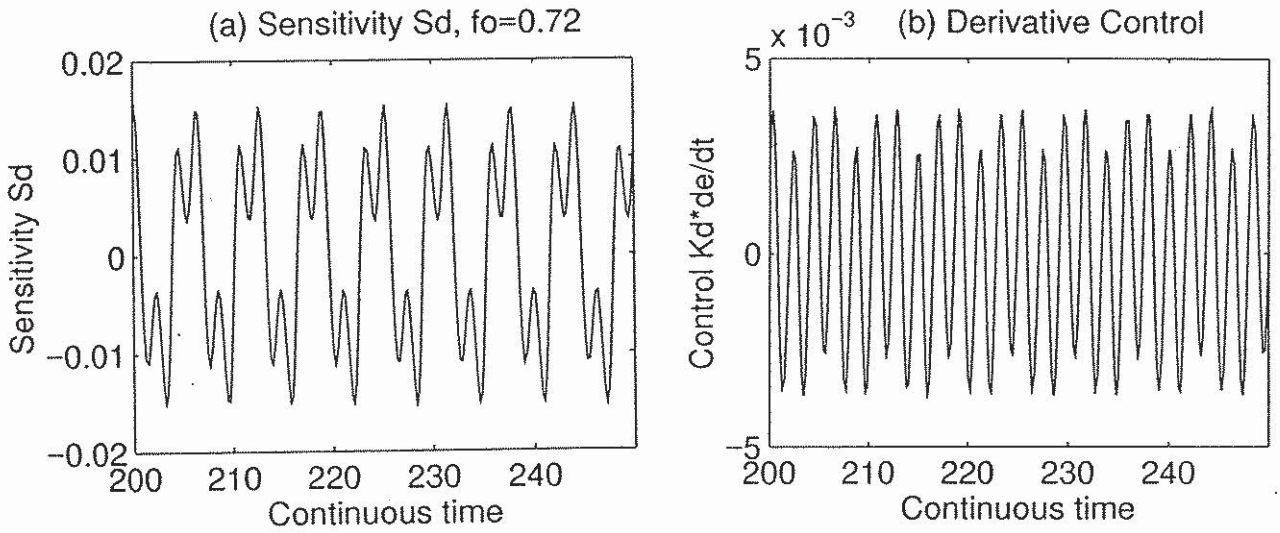

Fig.6: (a) Derivative sensitivity function $S_d(t)$ and (b) the derivative control K_d e'.

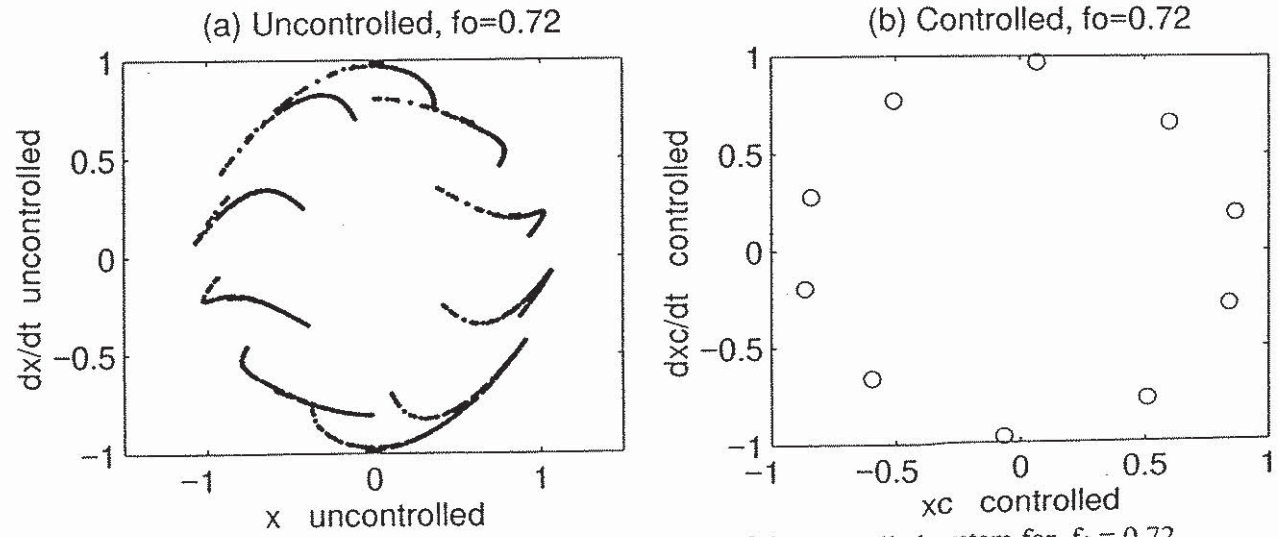

Fig.7: (a) Poincare map of the uncontrolled system and (b) of the controlled system for $f_0 = 0.72$.

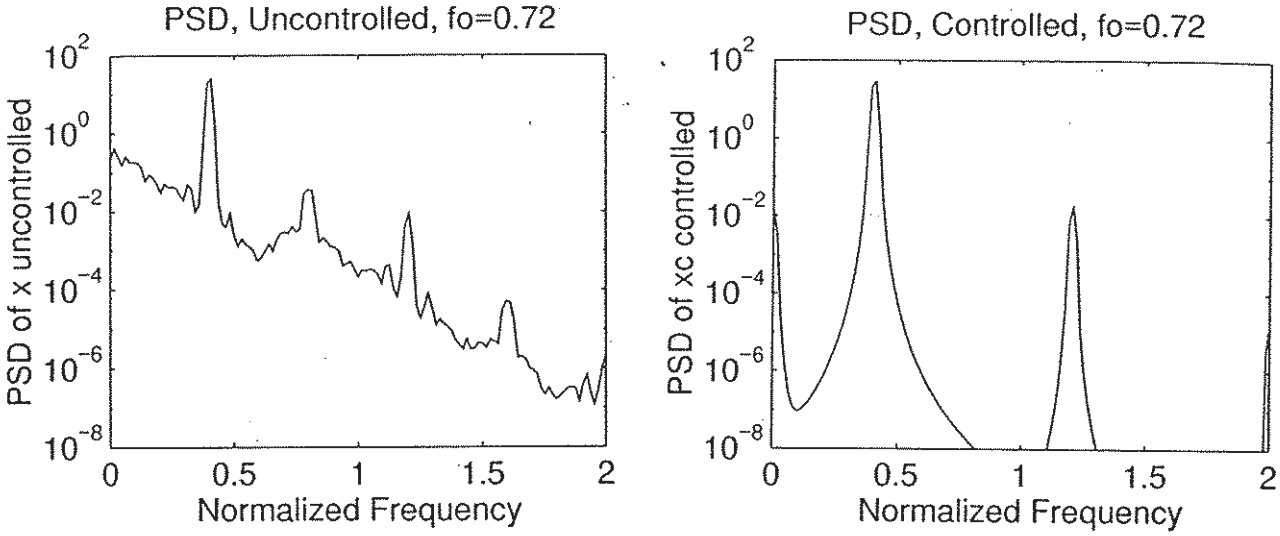

Fig.8: (a) Power spectral density (PSD) of the uncontrolled system and (b) of the controlled system.

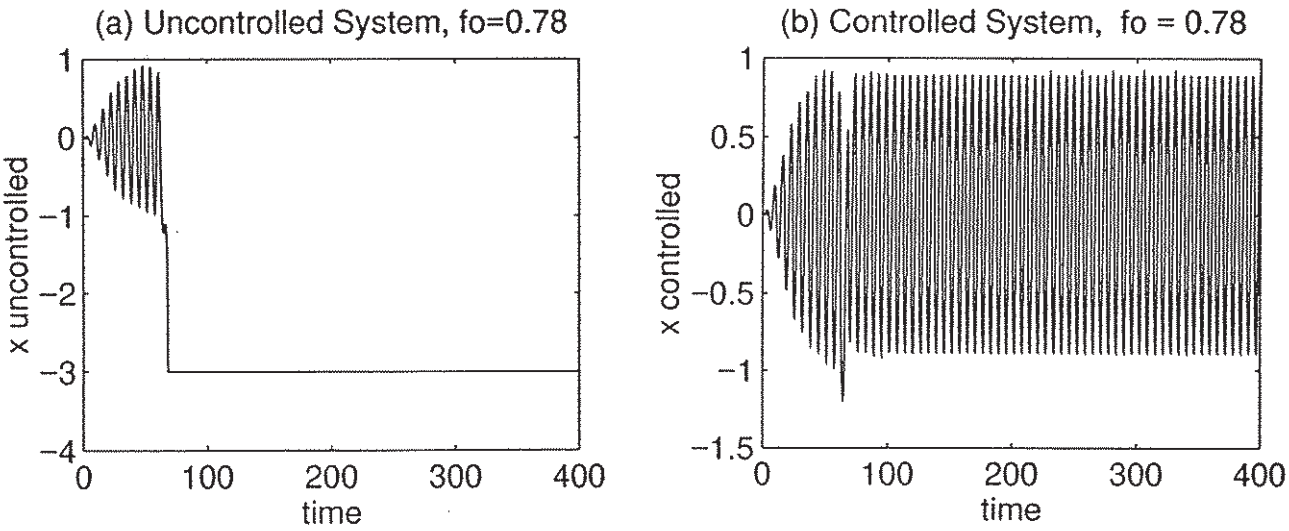

Fig.9: (a) Crisis of the uncontrolled system and (b) the stabilized limit cycle motion of the controlled system.

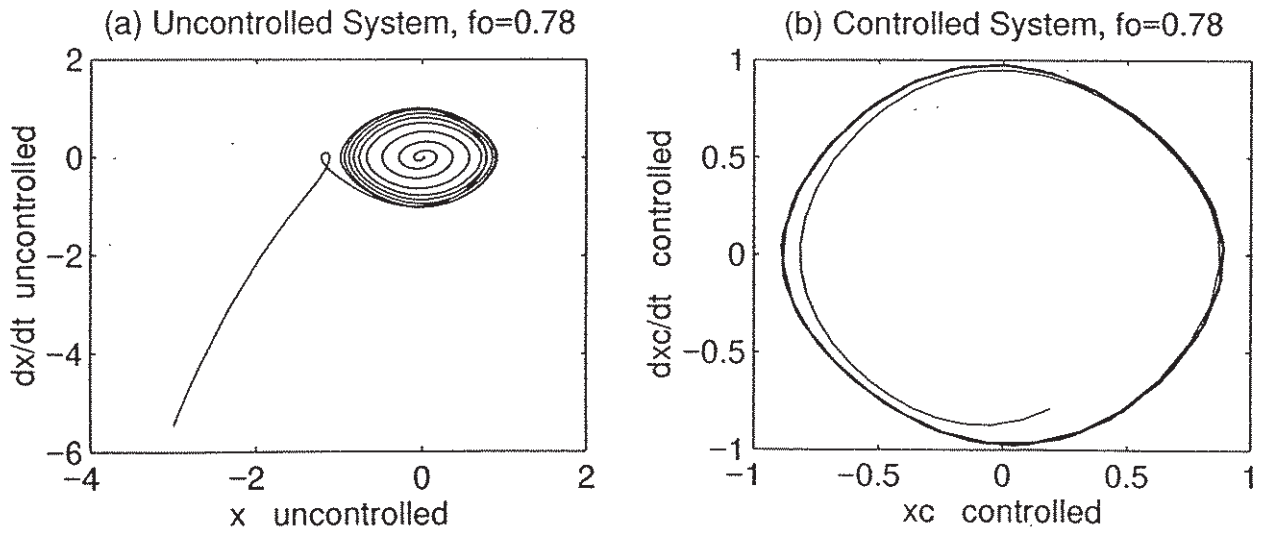

Fig.10: Phase portraits for $f_0 = 0.78$: (a) Crisis and escape from the attractor for the uncontrolled system versus (b) near limit cycle when the adaptive control is applied.